Proc. Natl. Acad. Sci. USA
Vol. 92, pp. 6097–6101, June 1995
Biochemistry

Synthesis of a thymidyl pentamer of deoxyribonucleic guanidine and binding studies with DNA homopolynucleotides

(antisense/antigene/hybrid duplex/triple helix)

ROBERT O. DEMPCY, KENNETH A. BROWNE, AND THOMAS C. BRUICE

Department of Chemistry, University of California, Santa Barbara, CA 93106

Contributed by Thomas C. Bruice, March 13, 1995

ABSTRACT **Replacement of the phosphodiester linkages of the polyanion DNA with guanidine linkers provides the polycation deoxynucleic guanidine (DNG). The synthesis of pentameric thymidyl DNG is provided. This polycationic DNG species binds with unprecedented affinity and with base-pair specificity to negatively charged poly(dA) to provide both double and triple helices. The dramatic stability of these hybrid structures is shown by their denaturation temperatures (T_m). For example, the double helix of the pentameric thymidyl DNG and poly(dA) does not dissociate in boiling water (ionic strength = 0.12), whereas the T_m for pentameric thymidyl DNA associated with poly(dA) is ≈13°C (ionic strength = 0.12). The effect of ionic strength on T_m for DNG complexes with DNA shows an opposite correlation compared with double-stranded DNA and is much more dramatic than for double-stranded DNA.**

The design of therapeutic oligonucleotides capable of inhibiting cellular processes at the translational or transcriptional level forms the basis of antisense/antigene technology. This exciting new class of drug design takes advantage of the specific hydrogen-bonding interactions (Watson–Crick and Hoogsteen base pairs) between complementary oligonucleotides, resulting in antisense/antigene agents with remarkable specificity for target RNA/DNA. Key goals in the design of modified oligonucleotides include (*i*) increased binding affinity with retention of binding specificity, (*ii*) resistance to degradation by nucleases, and (*iii*) increased membrane permeability.

In recent years, much attention has focused on the development of antisense agents that replace the negatively charged 5′–3′ phosphodiester linkage found in natural nucleic acids with a neutral backbone moiety [e.g., amide, methylene (methylimino), formacetal, etc. (1)]. In general, this strategy has produced interesting results. For example, increased binding affinities to DNA [evidenced by ≈0.1–3°C per linkage increase in strand denaturation temperature (T_m)] result from the absence of electrostatic repulsions between strands; these synthetically modified oligonucleotides are resistant to nuclease degradation but suffer as antisense agents, unfortunately, from lack of solubility.

We previously reported the synthesis of the positively charged thymidyl deoxyribonucleic guanidine (DNG) dinucleotide and provided modeling studies involving oligomeric DNG complexed with DNA (2). The distinctive structural feature of DNG is the replacement of the negatively charged DNA phosphate bridge with a positively charged asterogenic 5′–3′ guanidyl linkage. Thus, in addition to Watson–Crick base-pair-binding interactions, DNG also provides electrostatic binding interactions with phosphate linkages of the target nucleic acid.

Molecular modeling studies of the double-stranded DNG·DNA [$d(gT)_{10}$·$d(pA)_{10}$] and the triple-helical hybrids [$d(pT)_{10}$·$d(pA)_{10}$·$d(gT)_{10}$] and [$d(gT)_{10}$·$d(pA)_{10}$·$d(gT)_{10}$] suggested that the guanidyl (g) backbone in DNG was a viable alternative to the phosphodiester linkages of DNA (2). DNG should be stable *in vivo* because the guanidyl linkage is not labile to cellular nucleases nor chemical degradation under physiological conditions. Finally, a DNG·DNA complex will exist with a net neutral charge; this might be anticipated to facilitate cellular uptake. A major concern of ours, however, was the possibility that the electrostatic attraction between the guanidyl and phosphate moieties could be *so* great that DNG would not be specific for its complementary sequence of DNA or RNA.

The specific features of the DNG model prompted us to devise methods useful in the synthesis of oligomeric DNG. We report here the synthesis of pentameric thymidyl DNG (**1**) and provide results which demonstrate that **1** forms unusually stable complexes with poly(dA) but does not form detectable structures with homopolymers of the other deoxyribonucleic acids.

MATERIALS AND METHODS

General Procedures. All TLC was run with Merck silica gel (F_{254}) plates. ^{1}H NMR were obtained on Varian Gemini-200 or General Electric GN-500 spectrometers in dimethyl sulfoxide-d_6 at 25°C unless otherwise specified. Chemical shifts (ppm) were referenced to dimethyl sulfoxide (2.49 ppm). Purified DNA oligonucleotides were purchased from the University of California at San Francisco Biomolecular Resource Center and from Pharmacia. The concentrations of DNA and DNG oligonucleotide stock solutions were determined at 67°C with a Cary-14 UV/vis spectrophotometer from the Beer–Lambert law by using known extinction coefficients for individual nucleotides at 260 nm (3). Mass spectra were obtained from the mass spectrometry laboratory of the University of California, Los Angeles. The following nomenclature is used: the guanidyl linkage of DNG oligonucleotides is specified by the letter g, whereas thiourea-linked oligonucleotides are specified by the letter t.

Synthesis. *3′-Azido-5′-isothiocyano-3′,5′-deoxythymidine (**2**; Fig. 1).* To a suspension of 5′-amino-3′-azido-3′,5′-deoxythymidine (2) (2.0 g, 6.60 mmol) in 200 ml of dry methylene chloride, 2.0 ml of dry triethylamine was added followed by carbon disulfide (20 ml) and 1,3-dicyclohexylcarbodiimide (1.48 g, 7.17 mmol). The resulting solution was stirred at room temperature for 30 min and then evaporated to dryness *in vacuo*. The residue was dissolved in a minimum volume of ethyl acetate and chromatographed through a silica gel column eluting with ethyl acetate. The product fractions were evaporated to afford a homogenous oil: yield, 1.62 g (79%); TLC (ethyl acetate) R_f = 0.66; IR (NaCl plate) 3192, 3047, 2930, 2106, 1699, 1470, 1271, 1084 cm^{-1}; ^{1}H NMR δ 7.45 (1 H, s, 6-H), 6.17 (1 H, t, J = 6.7 Hz, 1′-H), 4.48 (1 H, m, 3′-H), 4.02

The publication costs of this article were defrayed in part by page charge payment. This article must therefore be hereby marked "*advertisement*" in accordance with 18 U.S.C. §1734 solely to indicate this fact.

Abbreviations: DNG, deoxyribonucleic guanidine; DMF, *N,N*-dimethylformamide.

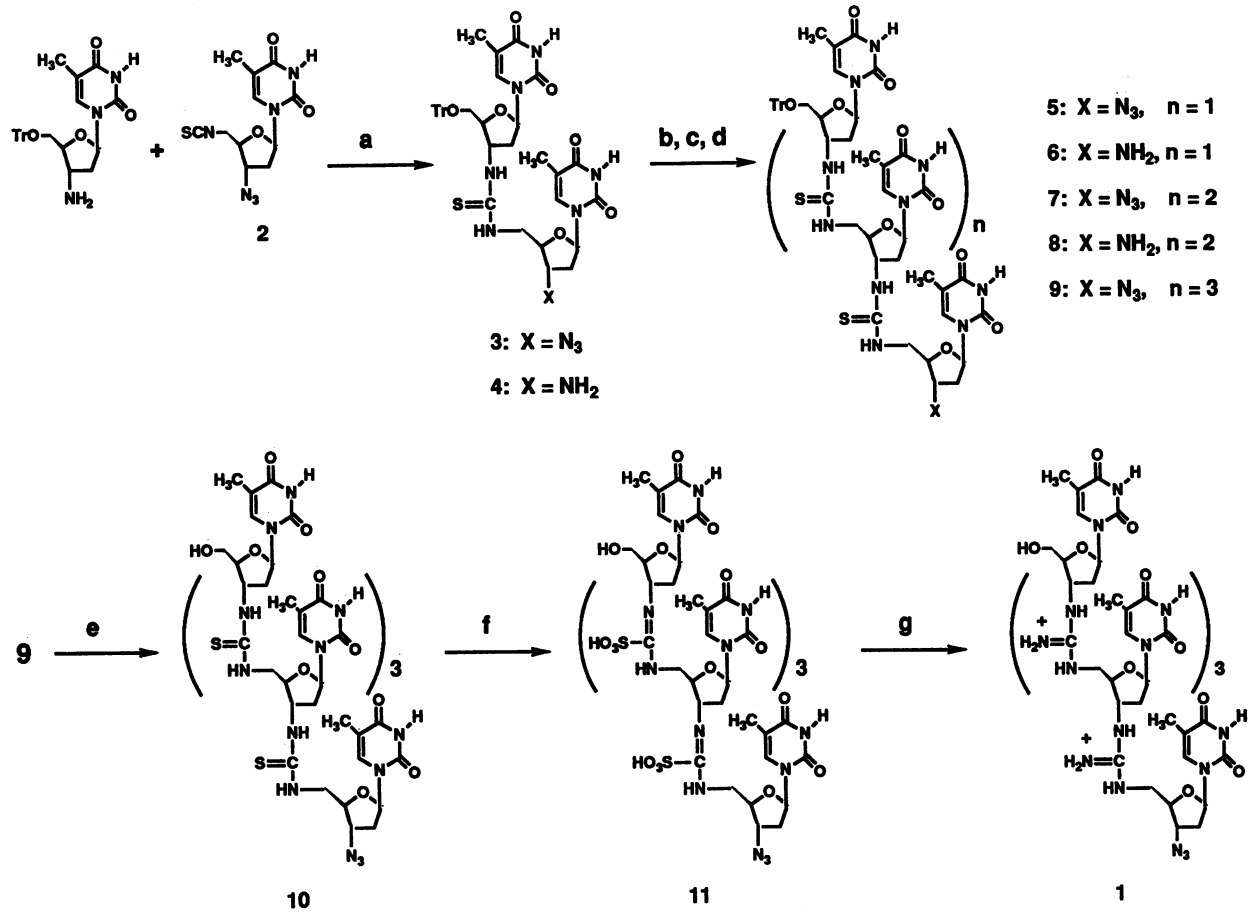

FIG. 1. Steps: a, *N,N*-dimethylformamide (DMF); b, H_2S (g), aqueous pyridine; c, **2**, DMF; d, steps b and c: two cycles; e, CF_3COOH; f, peracetic acid; g, NH_4OH.

(3 H, m, 4'-H and 5'-Hs), 2.43 (2 H, m, 2'-Hs), 1.82 (3 H, s, methyl protons); HRMS (chemical ionization) *m/e* 309.0759 $(M + H)^+$, calcd. for $C_{11}H_{13}N_6O_3S$ 309.0769.

Trityl-d(T$_t$T)-azido (**3**). A solution of **2** (1.18 g, 3.85 mmol) and 5'-*O*-trityl-3'-amino-3'-deoxythymidine (**4**) (1.86 g, 3.85 mmol) in 15 ml of dry *N,N*-dimethylformamide (DMF) was stirred for 3.0 hr at 80°C. The solution was evaporated to dryness, and the residue was precipitated from ethyl acetate ether: yield, 2.60 g (85%); m.p. 148°C (dec); TLC (10% methanol in ethyl acetate) R_f = 0.48; IR (KBr) 3344, 3059, 2105, 1697, 1471, 1270, 1079, 705 cm^{-1}; ^1H NMR δ 7.65–7.10 (17 H, m, 6-Hs and trityl protons), 6.22 and 6.11 (2 H, 2 × t, *J* = 6.74 and 6.74 Hz, 1'-Hs), 4.44–3.09 (8 H, 3'-, 4'-, and 5'-Hs), 2.48–2.12 (4 H, 2 × m, 2'-Hs), 1.81 and 1.40 (6 H, 2 × s, methyl protons); HRMS [fast-atom bombardment (FAB)] *m/e* 792.2934 $(M + H)^+$, calcd for $C_{40}H_{42}N_9O_7S$ 792.2928.

Trityl-d(T$_t$T)-amino (**4**). A thin stream of hydrogen sulfide gas was bubbled into a solution of **3** (2.50 g, 3.16 mmol) in 50% (vol/vol) aqueous pyridine (80 ml) at room temperature for 3.0 hr. The solution was filtered, and the filtrate was evaporated to dryness. The residue was precipitated from ethyl acetate ether: yield, 2.21 g (91%); m.p. 152°C (dec); TLC (1-butanol/water/acetic acid, 5:3:2) R_f = 0.48; IR (KBr) 3060, 3035, 2927, 1699, 1544, 1473, 1448, 1269, 1076, 769, 706 cm^{-1}; ^1H NMR δ 7.55–7.26 (17 H, m, 6-Hs and trityl protons), 6.18 (2 H, m, 1'-Hs), 4.00–3.13 (8 H, 3'-, 4'-, and 5'-Hs), 2.24–1.96 (4 H, m, 2'-Hs), 1.80 and 1.40 (6 H, 2 × s, methyl protons); HRMS (FAB) *m/e* 766.3057 $(M + H)^+$, calcd for $C_{40}H_{44}N_7O_7S$ 766.3023.

Trityl-d(T$_t$)$_2$T-azido (**5**). A solution of **4** (1.16 g, 1.52 mmol) and **2** (0.515 g, 1.67 mmol) was stirred in dry DMF for 4.0 hr at 80°C. The solution was evaporated to dryness, and the residue was precipitated from ethyl acetate ether: yield, 1.31 g (80%); m.p. 180°C (dec); TLC (1-butanol/water/acetic acid, 5:3:2) R_f = 0.77; IR (KBr) 3060, 2106, 1697, 1545, 1475, 1449, 1365, 1270, 1083 cm^{-1}; ^1H NMR δ 8.00–7.22 (18 H, 6-Hs and trityl protons) 6.18 and 6.083 (3 H, m and t, *J* = 6.5 Hz for t, 1'-Hs) 5.08–3.37 (12 H, 3'-, 4'-, and 5'-Hs), 2.46, 2.31, and 2.18 (6 H, 3 × m, 2'-Hs), 1.81, 1.80, and 1.45 (9 H, 3 × s, methyl protons); HRMS (FAB) *m/e* 1074.3734 $(M + H)^+$, calcd for $C_{51}H_{56}N_{13}O_{10}S_2$ 1074.3714.

Trityl-d(T$_t$)$_4$T-azido (**9**). Hydrogen sulfide gas was bubbled into a solution of **5** (1.31 g, 1.22 mmol) in 40 ml of 50% (vol/vol) aqueous pyridine for 4.0 hr. The reaction solution was filtered, and the filtrate was evaporated affording the amine (**6**) [TLC (1-butanol/water/acetic acid, 5:3:2) R_f = 0.57], which was dissolved in 15 ml of dry DMF containing **2** (451 mg, 1.46 mmol). A few drops of triethylamine were added to neutralize trace amounts of acid. The solution was stirred at 65°C for 4.0 hr, after which the solvent was evaporated. The residue was triturated with 50 ml of hot methanol. After cooling the mixture to room temperature, 50 ml of ether was added. The precipitate (**7**) was collected: yield, 1.38 g (84%) for the two-step process: TLC (1-butanol/water/acetic acid, 5:3:2) R_f = 0.74.

The solid tetramer **7** from above was dissolved in 30 ml of 50% (vol/vol) aqueous pyridine, and the azido moiety was reduced as described above for compound **5**. The resulting amine **8** was dissolved in 20 ml of dry DMF containing **2** (451 mg, 1.46 mmol) and stirred at 65°C for 4.0 hr. After evaporating the DMF, the residue was precipitated from DMF/methanol: yield, 1.41 g (84%) for the two-step reduction/coupling process; m.p. > 200°C (slow dec); TLC (1-butanol/water/acetic acid, 5:3:2) R_f = 0.74; IR (KBr) 3061, 2107, 1704,

1552, 1472, 1270, 1090, 769, 706 cm^{-1}; ^1H NMR (50°C) δ 7.98–7.22 (20 H, 6-Hs and trityl protons), 6.22–6.07 (5 H, m and t, J = 6.5 Hz for the t, 1′-Hs), 5.07–3.18 (20 H, 10 × m, 3′-, 4′-, and 5′-Hs), 2.40–2.10 (10 H, 4 × m, 2′-Hs), 1.81, 1.79, and 1.43 (15 H, 3 × s, methyl protons); MS (FAB) m/e 1638 $(M + H)^+$, calcd for $C_{73}H_{84}N_{21}O_{16}S_4$ 1638.

d(T$_t$)$_4$T-azido (**10**). A solution of **9** (220 mg, 0.134 mmol) in 8.0 ml of 30% (vol/vol) trifluoroacetic acid in methylene chloride was stirred at room temperature for 15 min. Methanol (12 ml) was added, and the crystals that formed were collected and rinsed with isopropanol: yield, 163 mg (87%); m.p. > 200°C (slow dec); TLC (1-butanol/water/acetic acid, 5:3:2) R_f = 0.70; IR (KBr) 3331, 3065, 2107, 1704, 1553, 1473, 1366, 1271, 1088, 772 cm^{-1}; ^1H NMR δ 7.77, 7.52, 7.48, and 7.46 (5 H, 4 × s, 6-Hs), 6.23–6.06 (5 H, m, 1′-H), 5.10–3.44 (21 H, 5′-OH, 3′-, 4′-, and 5′-Hs), 2.4–2.1 (10 H, m, 2′-Hs), 1.80 and 1.77 (15 H, 2 × s, methyl protons); HRMS (FAB) m/e 1396.4207 $(M + H)^+$, calcd for $C_{54}H_{70}N_{21}O_{16}S_4$ 1396.4192.

d(Tg)$_4$T-azido (**1**). Compound **10** (40 mg, 0.0287 mmol) was added to 0.5 ml of peracetic acid solution [32% (wt/wt) in dilute acetic acid, Aldrich] previously cooled to 0°C. The resulting solution was stirred for 15 min at 0°C. Methanol (4.0 ml) was added, and the crystals of **11** that formed were collected and rinsed with methanol: yield, 43 mg (94%). Thirty milligrams of **11** (0.0189 mmol) was dissolved in 1.0 ml of concentrated ammonium hydroxide and stirred in a sealed tube at 65°C for 14 hr. The white crystals that formed were collected and rinsed with water: yield, 24 mg (77%). Conversion of **1** into its water-soluble hydrochoride salt form was accomplished by suspending **1** in water and adding dilute HCl solution until the sample dissolved. An analytical sample was prepared by preparative HPLC using an Alltech WCX cation-exchange column using 0.80 M ammonium acetate buffer, pH 5.0, as the mobile phase. The major component was isolated, and ammonium acetate was removed from the DNG sample by repetitive evaporations from water; m.p. > 150°C (slow dec); IR (KBr) 3356, 3211, 2966, 2826, 2108, 1674, 1502, 1467, 1355, 1090, 789 cm^{-1}; ^1H NMR (^2H_2O) δ 7.79, 7.62, and 7.60 (5 H, 3 × s, 6-Hs), 6.32 and 6.25 (5 H, t and m, J = 5.5 Hz for the t, 1′-Hs), 4.78–3.70 (20 H, 3′-, 4′-, and 5′-Hs), 2.93–2.50 (10 H, 3 × m, 2′-Hs), 2.06 (15 H, s, methyl protons). The guanidyl carbons are observed between 156.46 and 156.41 ppm in the ^{13}C NMR spectrum (^2H_2O); MS (FAB) m/e 1328.60 $(M + H)^+$, calcd for $C_{54}H_{74}N_{25}O_{16}$ 1328.56.

Electrophoresis. The electrophoretic mobilities of the DNG oligonucleotides d(Tg)$_4$T-azido (**1**) and d(TgT)-azido (2) and the DNA oligonucleotides d(TpT) and d(Tp)$_4$T (1–2 × 10^{-7} mol in bases, each) were compared on a 4.5% D600 (a proprietary acrylamide polymer solution of AT Biochem) horizontal gel (0.088 M NH_4OAc, pH 5.8). The oligonucleotides were electrophoresed through this medium in its polymerized form for 2 hr at a constant 1.5 V/cm. The separated oligonucleotides were observed by "UV-shadowing" on an ultraviolet transilluminator emitting at 254 nm.

Thermal Denaturation Studies. Plots of A_{260} vs. T (°C) for **1** in the presence of poly(dA), p(dG)$_{12-18}$, poly(dI), poly(dC), or poly(dT) were obtained at pH 7.0 (0.01 M K_2HPO_4) using a Perkin–Elmer UV/vis spectrophotometer in conjunction with a National Institute of Standards and Technology digital thermometer (accurate to ± 0.2°C). The concentration of each of the oligonucleotides was 4.17 × 10^{-5} M in bases. The ionic strength (μ) of samples was adjusted with an appropriate concentration of KCl. In a typical experiment, a solution of **1** and a DNA oligomer were heated to 93°C and allowed to cool to 5°C over several hours. Data points were then collected as the temperature was raised at the rate of ≈1°C per 5 min. The data points that comprise each curve were then computer fitted to Eq. **1** (one hyperchromic transition) or Eq. **2** (two hyperchromic transitions),

$$A_{260} = \frac{a_1}{1 + e^{b_1(T - T_{m1})}} + d \quad [1]$$

$$A_{260} = \frac{a_1}{1 + e^{b_1(T - T_{m1})}} + \frac{a_2}{1 + e^{b_2(T - T_{m2})}} + d, \quad [2]$$

which optimize for the inflection points of a curve (T_{m1} and T_{m2} in the case of DNG), the change in absorbances between inflection points (a_1 and a_2), the slope coefficients (b_1 and b_2), and the absorbance at high temperature (d).

RESULTS AND DISCUSSION

Synthesis. In a previous report (2) we described the synthesis of the thymidyl DNG dimer via a condensation reaction between 3′-amino-3′-deoxythymidine and 3′-azido-5′-*S*-methylisothiouronium-3′,5′-deoxythymidine. Chain extension from the dimer was proposed to follow a cyclic two-step process involving reduction of the 3′-azido moiety to the amine, followed by another condensation reaction. Although this synthetic strategy succeeded in affording the DNG trimer [d(T$_g$)$_2$T-azido], attempts to synthesize longer chains were unsuccessful. The polar and organic-solvent-insoluble nature of the growing cationic chain rendered purification of desired oligomers exceedingly difficult. To overcome this problem, another synthetic route was developed, in which a pentameric thymidine oligomer was constructed with a neutral 5′–3′ thiourea backbone (Fig. 1) via a cyclic process. Thus, the reaction between 3′-amino-5′-*O*-trityl-3′-deoxythymidine [(4); the 3′-azido analogue in ref. 4 was reduced with Pd/C, H_2(g) in ethanol] and the 5′-isothiocyano derivative (**2**) afforded the thiourea-linked dimer (**3**). Reduction of the 3′-azido moiety with hydrogen sulfide in aqueous pyridine yielded the dimer amine (**4**). Condensation of **4** with a slight excess of **2** produced the chain-extended oligomer (**5**). Two additional rounds of the reduction/condensation cycle afforded the desired pentameric oligomer (**9**). The thiourea backbone was then converted to a guanidyl backbone by a two-step process involving oxidation of the thiourea linkages with peracetic acid [forming the amino-iminosulfonic acid derivative (**11**)] followed by amidation, forming the DNG oligomer (**1**).

Electrophoresis. The electrophoretic behavior of DNG migrating through a polyacrylamide gel was compared to the migration of DNA (Fig. 2). The respective oligomers migrate in opposite directions. Both dimeric and pentameric DNG molecules migrate toward the cathode while the analogous

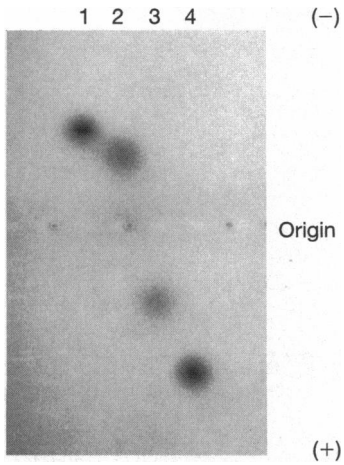

FIG. 2. Electrophoretic mobilities of the DNG oligonucleotides d(Tg)$_4$T-azido (**1**) and d(TgT)-azido (lanes 1 and 2) and the DNA oligonucleotides d(TpT) and d(Tp)$_4$T (lanes 3 and 4). Between 1 and 2 × 10^{-7} mol (in bases) of each oligonucleotide were loaded into adjacent wells in the center (Origin) of the gel.

DNA oligonucleotides travel toward the anode, the longer oligonucleotides migrating at a faster rate. This difference is as expected for molecules that are essentially identical except for net charge (e.g., +4 vs. −4 for **1** and $d(Tp)_4T$, respectively). The relative magnitudes of migration are similar, although not the same, for DNG and DNA with the same number of bases. This slight discrepancy could be due to the increased rigidity of the guanidyl vs. the phosphodiester backbone or to the mass of the phosphate moiety, which is 38 Da greater per linkage than a guanidyl linkage. Because the oligonucleotides are migrating mainly by charge, the difference in mass between DNG and DNA should have a negligible influence on their relative electrophoretic migrations. Thus, the difference in oligonucleotide backbone flexibility is likely the main factor in the different migration of DNG vs. DNA.

Thermal Denaturation Studies. In the thermal denaturation analysis of **1** bound to poly(dA), two distinct hyperchromic shifts were observed in the UV spectra (μ = 0.22, 0.62, and 1.2; Fig. 3*A*). In analogy to DNA and RNA thermal denaturation analysis (5), these transitions correspond to the denaturation of a triple-helical hybrid at 68, 41, and 36°C followed by denaturation of a duplex at 79, 70, and 71°C. At μ = 0.12, only one transition was seen centered at 85°C; the thermal stability is apparently so great that the duplex structure does not denature at near boiling temperatures. This result contrasts with the denaturation profiles of $d(T_p)_{15}T$ bound to poly(dA); all have sharp, single denaturation transitions from duplex to single strands of DNA (39, 41, 52, and 56°C at μ = 0.12, 0.22, 0.62, and 1.2, respectively; plots not shown). There was no hyperchromic shift in the UV spectra of a solution between ≈5° and 93°C, which contained **1** and $p(dG)_{12-18}$, poly(dI), poly(dC), or poly(dT) (examined at both μ = 0.12 and 1.2, pH 7.0; Fig. 3*B*) that could be attributed to denaturation of a complex with **1** [although there was a hyperchromic shift centered at ≈40°C that was due to the denaturation of a poly(dC) complex with itself; this phenomenon has been reported (6)]. This result is evidence against DNG binding to DNA in a nonspecific manner. Therefore, we conclude that electrostatic interactions dramatically increase the binding affinity of DNG to DNA without compromising Watson–Crick and Hoogsteen base-pair-binding interactions.

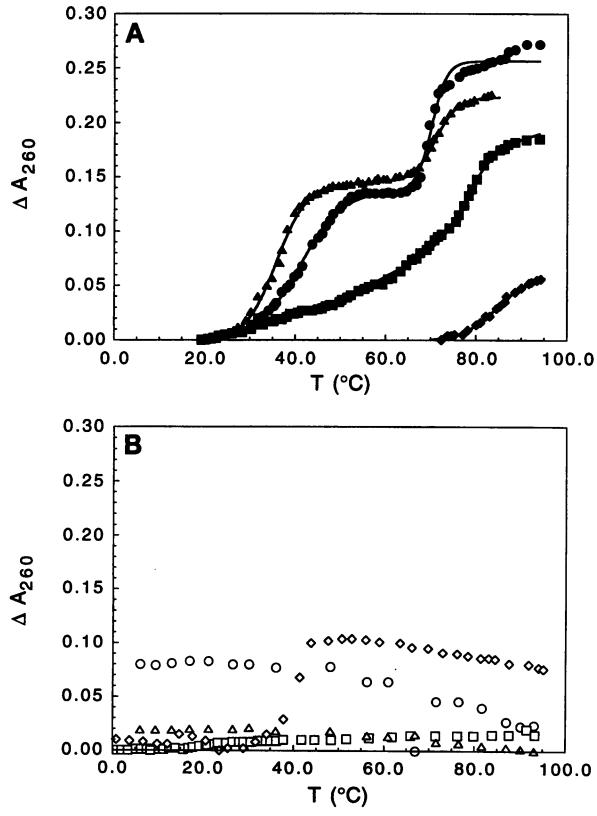

FIG. 3. (*A*) Plots of the change of A_{260} vs. T (°C) for $d(Tg)_4T$-azido (**1**) in the presence of poly(dA) at pH 7.0 (0.01 M K_2HPO_4). Ionic strength (μ) was held constant at 0.12 (◆), 0.22 (■), 0.62 (●), and 1.20 (▲) with KCl. (*B*) Plots of the change of A_{260} vs. T (°C) for **1** in the presence of $p(dG)_{12-18}$ (○), poly(dI) (□), poly(dC) (◇), or poly(dT) (△) are presented at μ = 1.2.

Ionic Strength-Dependency Studies. To compare our thermal denaturation results for DNG with results obtained for DNA and modified oligonucleotides, denaturation data were reduced to the unit terms of T_m per base pair and, similarly, T_m per linkage. The plot of T_m per base pair vs. ionic strength (Fig. 4) exemplifies the differences between the binding of DNG to DNA compared to the analogous DNA·DNA complex. Not only does thymidyl DNG have a tremendously greater affinity than thymidyl DNA for poly(dA) over a wide range of ionic strengths, but the effect of ionic strength is much more pronounced. Obviously, if electrostatic attraction stabilizes DNG·DNA complexes, the electrostatic force would be influenced by changing ionic strength. The observation that the effect of ionic strength has an opposite relationship for DNG complexes with DNA compared to DNA·DNA complexes is most noteworthy. Thus, while DNA·DNA duplexes become more stable with *increasing* ionic strength, triplexes and duplexes composed of both DNG and DNA become more stable with *decreasing* ionic strength. This result should be expected because (*i*) increased salt concentration will effectively mask the opposing rows of negative charges on double-stranded DNA, allowing a more stable duplex, and (*ii*) decreased salt concentration allows the oppositely charged backbones of the DNA hybrid complexes with DNG to be intimately salt paired, thus stabilizing these complexes. This effect has been alluded to with another positively charged oligonucleotide derivative (7) and suggests that electrostatic forces are responsible for the described binding affinity of DNG to DNA.

A few examples of positively charged oligonucleotides have appeared in recent literature. Both the (ethylmorpholino)phosphoramidite (7) and the (aminomethyl)phosphonate (8) oligonucleotide analogues contain positively charged ammonium groups connected via an alkyl linkage to the central phosphorous atom of the backbone moiety. DNG, on the other hand, maintains its positive charge in proper alignment to maximize its interaction with the backbone of the negatively

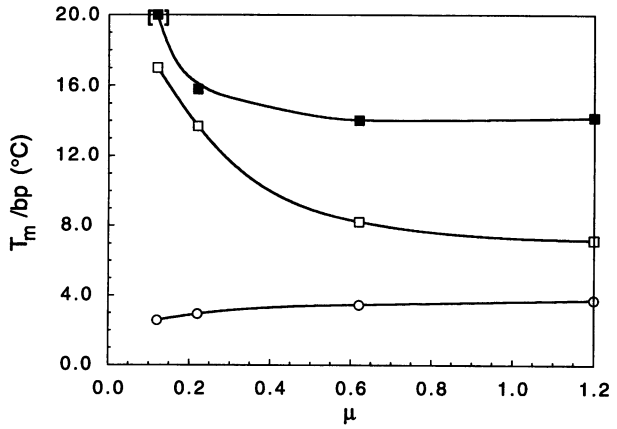

FIG. 4. Plot of T_m/(base pair) vs. ionic strength (μ) at pH 7.0 (0.01 M K_2HPO_4) from the denaturation of $d(Tg)_4T$-azido (□ and ■ for the first and second transitions, respectively) and $d(Tp)_{15}T$ (○) complexed to poly(dA). Ionic strengths were held constant by using 0.11, 0.21, 0.61, and 1.19 M KCl. The data point at the lowest ionic strength for the T_{m2} of DNG was simply taken as 100°C because no hyperchromic transition was apparent by 93°C.

charged phosphates of the opposite strand. Both the (ethylmorpholino)phosphoramidite and the (aminomethyl)phosphonate derivatives' dimeric complexes with DNA have T_m values in the range of 2–3°C per backbone linkage, whereas the corresponding thymidyl DNG complexes have T_m values of 14–>25°C per guanidyl linkage for duplex denaturation, depending on the salt concentration. Finally, the guanidyl linkage of DNG, unlike the linkages of the (ethylmorpholino)phosphoramidite and (aminomethyl)phosphonate oligonucleotides, is achiral. The importance of this point becomes apparent when considering the S_P and R_P stereoisomers of (aminomethyl)phosphonate oligonucleotides, which were shown to have vastly differing affinities for complementary DNA (8).

From the above discussion, the following conclusions can be drawn about DNG: (*i*) DNG has a positively charged backbone that differentiates it from DNA; (*ii*) thymidyl DNG is specific for its complementary adenyl tracts and not for guanyl or cytidyl tracts; (*iii*) due to electrostatic attractions, DNG binds to DNA with a much greater affinity than DNA to DNA or other known modified oligonucleotides to DNA; and (*iv*) the thermal stability of DNA hybrid structures with DNG is influenced by changing salt concentrations. At low ionic strength (μ = 0.12), short oligomers of DNG will essentially bind irreversibly to target nucleic acid. The specific properties of DNG warrant further investigation into its use as an antisense/antigene agent.

This study was supported by grants from the National Science Foundation and the Office of Naval Research.

1. Crooke, S. T. (1993) *FASEB J.* **7,** 533–539.
2. Dempcy, R. O., Almarsson, Ö. & Bruice, T. C. (1994) *Proc. Natl. Acad. Sci. USA* **91,** 7864–7868.
3. Beaven, G. H., Holiday, E. R. & Johnson, E. A. (1955) in *The Nucleic Acids: Chemistry & Biology, I,* eds. Chargaff, E. & Davidson, J. N. (Academic, New York), pp. 493–553.
4. Glinski, R. P., Khan, M. S., Kalamas, R. L. & Sporn, M. B. (1973) *J. Org. Chem.* **38,** 4299–4305.
5. Riley, M., Maling, B. & Chamberlin, M. J. (1966) *J. Mol. Biol.* **20,** 359–389.
6. Akinrimisi, E. O., Sander, C. & Ts'o, P. O. P. (1963) *Biochemistry* **2,** 340–344.
7. Letsinger, R. L., Singman, C. N., Histand, G. & Salunkhe, M. (1988) *J. Am. Chem. Soc.* **110,** 4470–4471.
8. Fathi, R., Huang, Q., Syi, J.-L., Delaney, W. & Cook, A. F. (1994) *Bioconjugate Chem.* **5,** 47–57.